Geochemical Journal, Vol. 52, pp. 69 to 74, 2018 doi:10.2343/geochemj.2.0497

NOTE

High-precision *in situ* analysis of Pb isotopes in melt inclusions by LA-ICP-MS and application of Independent Component Analysis

Morihisa Hamada,[1]* Jun-Ichi Kimura,[1] Qing Chang,[1] Takeshi Hanyu,[1] Takayuki Ushikubo,[2] Kenji Shimizu,[2] Motoo Ito,[2] Takahiro Ozawa[3] and Hikaru Iwamori[1,3]

[1]Department of Solid Earth Geochemistry, Japan Agency for Marine-Earth Science and Technology (JAMSTEC), 2-15 Natsushima-cho, Yokosuka, Kanagawa 237-0061, Japan
[2]Kochi Institute for Core Sample Research, Japan Agency for Marine-Earth Science and Technology (JAMSTEC), 200 Monobe-otsu, Nankoku, Kochi 783-8502, Japan
[3]Department of Earth and Planetary Sciences, Tokyo Institute of Technology, 2-12-1 Meguro-ku, Tokyo 152-8551, Japan

(*Received April 13, 2017; Accepted July 28, 2017*)

We report a high-precision ^{206}Pb-based lead isotope composition of olivine-hosted melt inclusions in basaltic rocks from Rarotonga Island, Polynesia, in the southern Pacific, using femtosecond laser ablation (FsLA)-multiple Faraday collector-inductively coupled plasma-mass spectrometry (MFC-ICP-MS). This improved method enables high-precision analysis of Pb isotopes from low-Pb (≤10 ppm) melt inclusions with a crater size of ~30 μm in diameter and depth. The small crater size allows for further analysis of major and trace elements from the same melt inclusions using FsLA-sector field (SF)-ICP-MS. Using Pb isotope ratios of two olivine-hosted melt inclusions, we suggest that the mantle source beneath Rarotonga Island is heterogeneous. Such identification becomes possible owing to high-precision *in situ* analysis of Pb isotopes in melt inclusions and application of statistical approaches such as Independent Component Analysis to the analytical data.

Keywords: Rarotonga Island, ocean island basalt, Pb isotope, laser ablation ICP-MS, Independent Component Analysis

Introduction

Radiogenic lead isotopes ^{206}Pb, ^{207}Pb, ^{208}Pb are useful to identify the isotopic diversity of the Earth's mantle, owing to (1) decay of radioactive ^{238}U, ^{235}U and ^{232}Th to grow Pb isotopes in the mantle, (2) intensive fractionation of U and Th from Pb via oceanic crust formation at mid-ocean ridges and formation of continental crust and residual slab in subduction zones, and (3) subsequent ingrowth of the recycled slab during prolonged storage and stirring in the mantle.

Secondary ion mass spectrometry (SIMS) has been a pioneering microanalytical technique of Pb isotopes over the past two decades (e.g., Saal *et al*., 2005; Yurimoto *et al*., 2004). Laser ablation-multiple collector-inductively coupled plasma-mass spectrometry (LA-MC-ICP-MS) has also been applied in the past decade (e.g., Paul *et al*., 2011). These microanalytical studies have revealed variations in Pb isotope ratios even within a single basalt lava specimen. The LA-MC-ICP-MS technique has been improved by using femtosecond laser ablation (FsLA; Kimura and Chang, 2012) and a multiple Faraday collector (MFC) equipped with high-gain Faraday amplifiers using a 10^{13} Ω resistor. The latter increases the signal/noise ratio of the target isotopes by ten times for a few ppm Pb compared with using a conventional 10^{11} Ω resistor, which enables one to determine the ^{206}Pb-based isotope ratios at a spatial resolution of a few tens of micrometers. It is difficult to analyze ^{204}Pb-based isotope ratios because the peaks of ^{204}Hg and ^{204}Pb overlap, which causes the analytical precision of ^{204}Pb to deteriorate (Kimura *et al*., 2016).

Here, we report the preliminary results of a high-precision microanalysis of Pb isotopes in olivine-hosted melt inclusions from Rarotonga Island by FsLA-MFC-ICP-MS. The reduced analytical area enabled the combined use of FsLA-sector field (SF)-ICP-MS for further analysis of major and trace elements from the same melt inclusions.

Samples

We analyzed two olivine-hosted melt inclusions recovered from enriched mantle EM1-type ocean island

*Corresponding author (e-mail: mhamada@jamstec.go.jp)

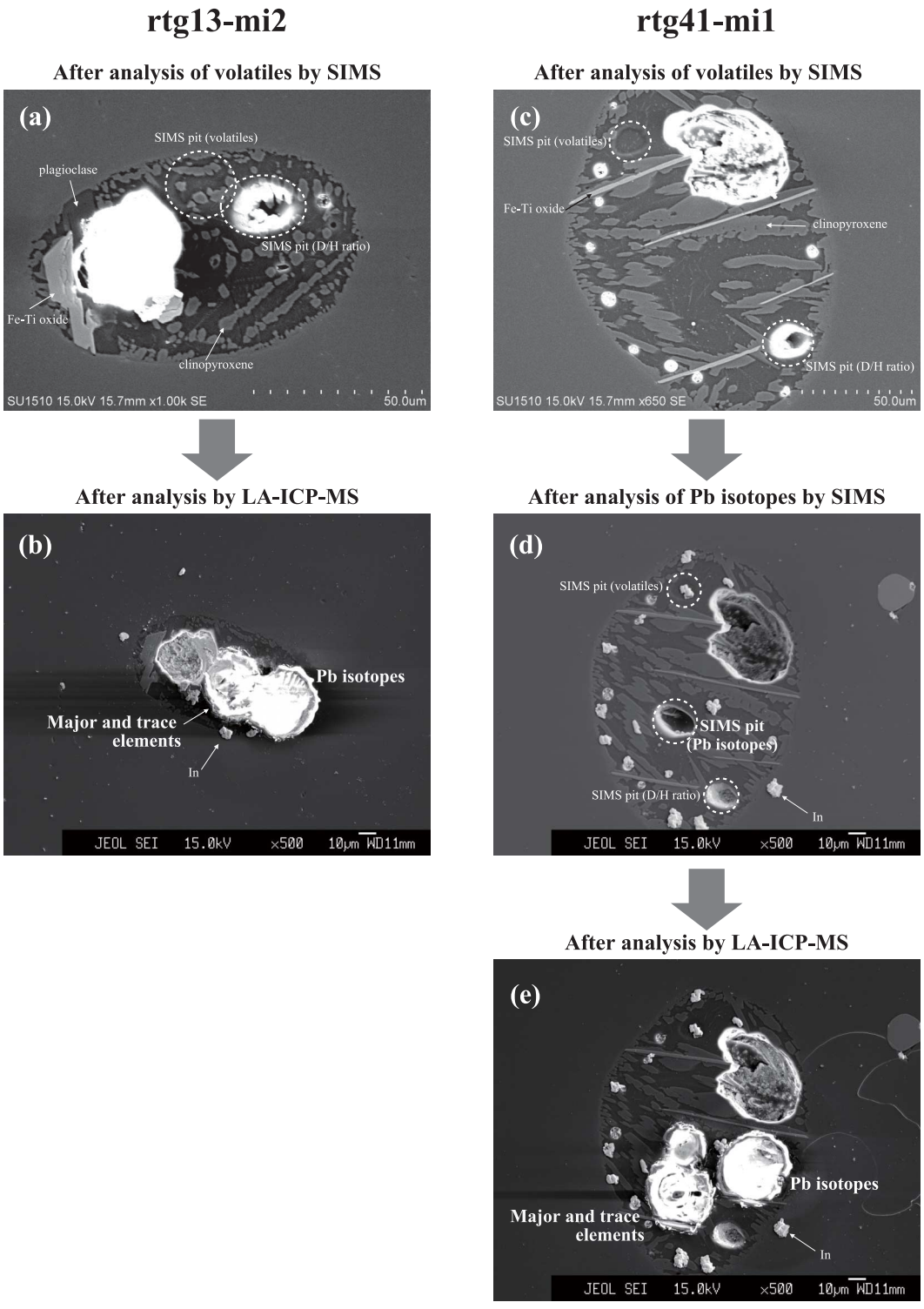

Fig. 1. Secondary electron images of studied melt inclusions. Metallic indium fragments (In) observed around the boundary of host olivine and melt inclusions are contamination from indium used for mounting, which occurred during preparation for secondary electron microscope (SEM) observation after SIMS analysis. Because these indium fragments contain a negligible amount of Pb, they cannot be contaminants of Pb (see Section "Analytical Methods" and Fig. S2 in Supplementary material 2). (a) Melt inclusion rtg13-mi2 after analysis of volatiles by SIMS. Fe-Ti oxide, plagioclase and clinopyroxene daughter minerals and two pits after SIMS analyses are indicated. (b) Melt inclusion rtg13-mi2 after laser ablation. (c) Melt inclusion rtg41-mi1 after analysis of volatiles by SIMS. Fe-Ti oxide and clinopyroxene daughter minerals and two pits after SIMS analyses are indicated. (d) Melt inclusion rtg41-mi1 after analysis of Pb isotopes by SIMS. (e) Melt inclusion rtg41-mi1 after laser ablation.

basalts (OIBs) from Rarotonga Island. The two melt inclusions, rtg13-mi2 and rtg41-mi1, suffered from post-entrapment overgrowth of the host olivines and crystallization of daughter minerals of clinopyroxene, plagioclase and Fe-Ti oxide implying slow cooling (Figs. 1a and 1c). Such melt inclusions are not ideal for determining the major, trace and volatile compositions of the original magma; however, they are still useful to determine the Pb isotope ratios of melts because the Pb isotope ratios are not affected by the post-entrapment processes.

Analytical Methods

The olivine crystals separated from the basaltic rocks were polished to expose melt inclusions. Multiple elements and Pb isotopes were analyzed by using four instruments: SIMS, an electron probe microanalyzer (EPMA), FsLA-MFC-ICP-MS, and FsLA-SF-ICP-MS. (1) Volatile elements and Pb isotope ratios were analyzed by a high-resolution SIMS (IMS-1280HR, Cameca, Paris, France) with a single-collection system at the Kochi Institute for Core Sample Research, at the Japan Agency for Marine-Earth Science and Technology (JAMSTEC) (Figs. 1a, 1c and 1d). We here report on only Pb isotope ratios. The analytical method is described in Supplementary material 1. (2) Major elements of the host olivines and melt inclusions were analyzed by EPMA (JXA-8500F, JEOL, Tokyo, Japan) at JAMSTEC. (3) We then analyzed the major and trace elements of the melt inclusions using SF-ICP-MS (Element XR, Thermo Fisher Scientific, Bremen, Germany) in combination with FsLA (OK-Fs2000K, OK Lab., Tokyo, Japan) at JAMSTEC (Kimura and Chang, 2012). A laser beam of 20 μm in diameter was used to analyze the volume-averaged mixture of the daughter minerals and the matrix glass. The depth of the ablation pit was <20 μm. We finally analyzed the Pb isotopes using the same FsLA connected to a modified high-sensitivity MFC-ICP-MS (Neptune, Thermo Fisher Scientific, Bremen, Germany) at JAMSTEC (Kimura *et al*., 2016). Following pre-ablation for 2 s to remove any remnants of surface Pb contamination, each melt inclusion was ablated at ~30 μm in diameter. The depth of the ablation pit was <30 μm (Figs. 1b and 1d). Negligible surface contamination is evidenced by the time resolving profiles of ^{208}Pb and the ^{208}Pb/^{206}Pb ratio (Supplementary Fig. S2). We analyzed the basalt standard of GSD-1G glass from the United States Geological Survey (USGS) for external calibration of FsLA-SF-ICP-MS and SRM 612 glass from the National Institute of Standard and Technology for standard bracketing correction in Pb isotope analysis by FsLA-MFC-ICP-MS. BHVO-2G glass from the USGS was analyzed for repeatability and laboratory bias tests in both elemental and Pb isotope analyses. Details of the analytical techniques, the repeatability and the laboratory bias are in Kimura and Chang (2012) and Kimura *et al*. (2016), and those for BCR-2G standard glass are given in Supplementary Table S1.

Results and Discussion

The analytical results of the two melt inclusions and the bulk-rock compositions of their host basalts (Hanyu *et al*., 2011) are listed in Supplementary Table S2. The incompatible trace element compositions normalized to the primitive mantle of Sun and McDonough (1989) are systematically higher than those of the bulk-rock composition of their host basalts (Fig. 2) because both melt inclusions are apparently more evolved than their hosts due to post-entrapment overgrowth of the host olivines. Highly incompatible elements in rtg13-mi2 are subparallel with those of the host basalt RTG301-1, except for Rb and Ba (Fig. 2a). In contrast, rtg41-mi1 shows relative depletions in mid to heavy rare earth elements (REEs) compared to its host basalt RTG305 (Fig. 2b).

We obtained ^{207}Pb/^{206}Pb = 0.8564 ± 0.0162 and ^{208}Pb/^{206}Pb = 2.121 ± 0.040 for rtg41-mi1 by SIMS (Fig. 3a; Table S2). Analytical errors (two-standard errors: 2SE) are determined by the statistics of secondary ion intensities, which is 19‰. We then obtained ^{207}Pb/^{206}Pb = 0.8355 ± 0.0015 and ^{208}Pb/^{206}Pb = 2.0888 ± 0.0026 for rtg13-mi2, and ^{207}Pb/^{206}Pb = 0.8504 ± 0.0029 and ^{208}Pb/^{206}Pb = 2.1078 ± 0.0035 for rtg41-mi1 by FsLA-ICP-MS (Fig. 3b; Table S2). Error ellipses show in-run uncertainties given by 2SE. The repeatability range is 1.2–2.7‰ (Table S1) and the analytical bias is in the same level with Kimura *et al*. (2016). The rtg13-mi2 and its host rock RTG301-1 have consistent ^{207}Pb/^{206}Pb whereas rtg13-mi2 shows lower ^{208}Pb/^{206}Pb than RTG301-1. The rtg41-mi1 shows higher ^{207}Pb/^{206}Pb and ^{208}Pb/^{206}Pb than its host rock RTG305 (Fig. 3a; Table S2). The Pb isotope ratios of rtg41-mi1 analyzed by SIMS and FsLA-MFC-ICP-MS are consistent, taking their errors into consideration (Fig. 3a). The error in the Pb isotope ratio of rtg41-mi1 by SIMS is comparable to those reported by Yurimoto *et al*. (2004) (Fig. 3b), although improvements have been made in analytical techniques and a present-day multi-collection SIMS has gained a factor of 2 in the precision of Pb isotope ratios (e.g., Rose-Koga *et al*., 2012). Owing to small errors of Pb isotope ratios by FsLA-MFC-ICP-MS, we now distinguish not only the difference in Pb isotope ratios between the two low-Pb melt inclusions (4.47 ppm for rtg13-mi2 and 11.55 ppm for rtg41-mi1) but also the difference in Pb isotope ratios between the melt inclusions and their host rocks.

In Fig. 3a, the two melt inclusions are plotted within a cloud of the bulk-rock data by Nakamura and Tatsumoto (1988). Actually, any binary plot for isotope ratios is too distorted to resolve the true data structure of terrestrial

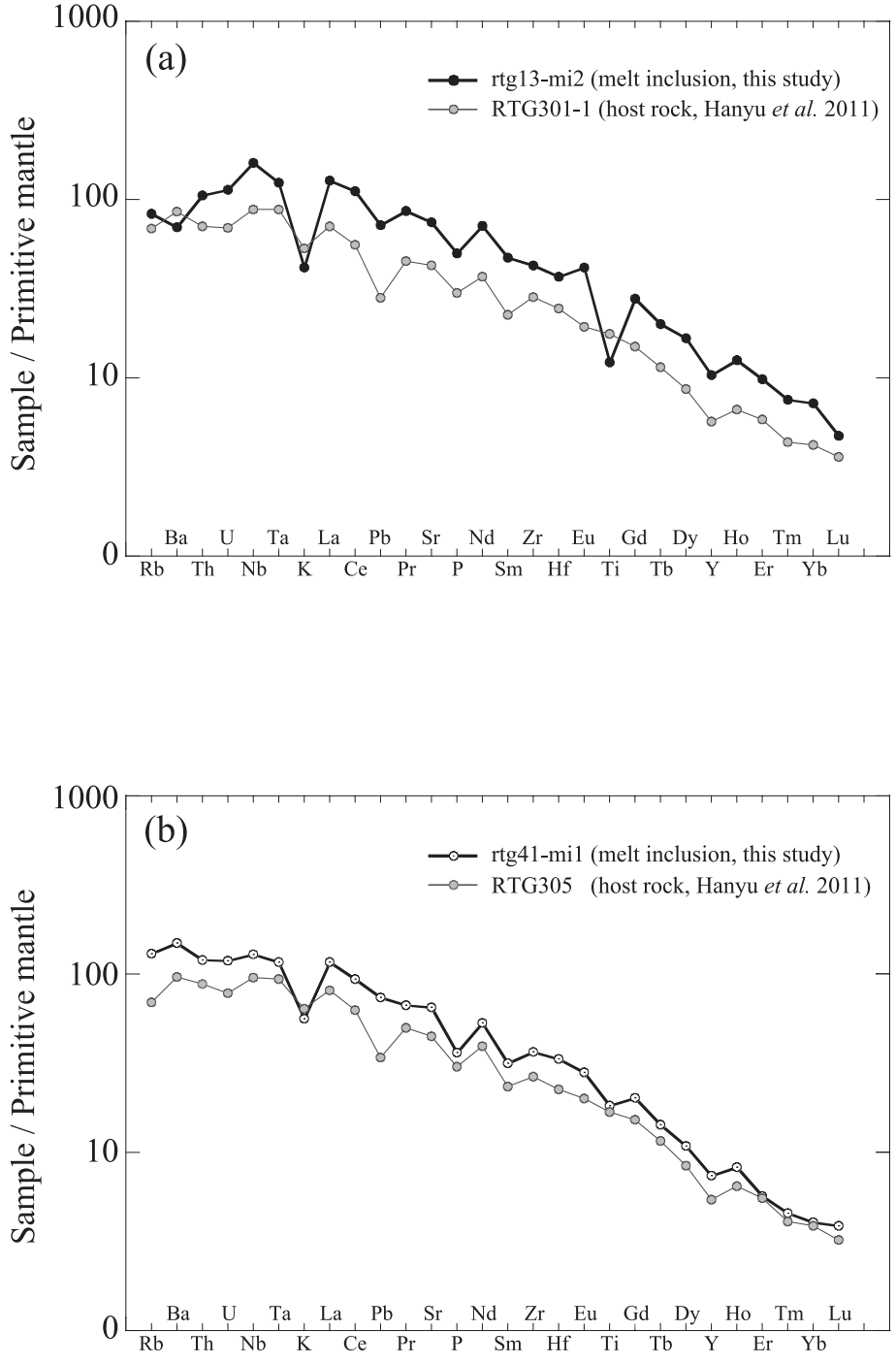

Fig. 2. Trace element compositions of olivine-hosted melt inclusions normalized to primitive mantle values from Sun and McDonough (1989). Trace element compositions of corresponding host rocks (Hanyu et al., 2011) are also plotted for comparison. (a) Trace element patterns of melt inclusion rtg13-mi2 and its host rock (RTG301-1). (b) Trace element patterns of melt inclusion rtg41-mi1 and its host rock (RTG305).

basalts (e.g., Iwamori and Nakamura, 2015). On the other hand, based on Independent Component Analysis (ICA) of the global basalt data for five isotope ratios of Sr, Nd and Pb, 95% of the isotopic variance is accounted for by only two independent components (IC1 and IC2) without losing essential information (Fig. 3c). The ICA simply resolves the data distribution, and individual ICs (i.e., IC1 and IC2) represent the statistical characteristic values of

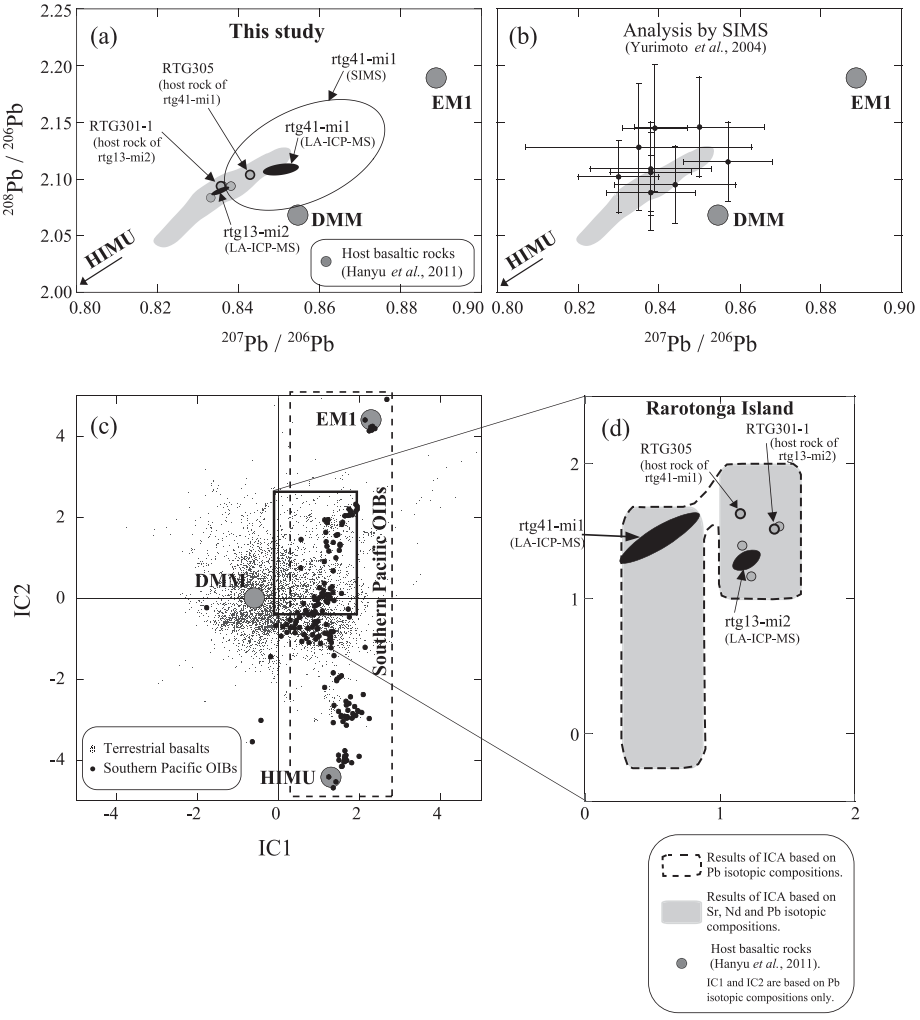

Fig. 3. Pb isotope composition of basaltic rocks and olivine-hosted melt inclusions from Rarotonga Island. (a) Results of this study. The rtg13-mi2 was analyzed by FsLA-MFC-ICP-MS. The rtg41-mi1 was analyzed by both FsLA-MFC-ICP-MS and SIMS. Error ellipses show in-run uncertainties given by two standard errors (2SE). Pb isotope compositions of bulk basaltic rocks from Rarotonga Island by Hanyu et al. (2011), including RTG301-1 (host rock of rtg13-mi2) and RTG305 (host rock of rtg41-mi1), are also plotted for comparison. The rtg13-mi2 and its host rock RTG301-1 have consistent $^{207}Pb/^{206}Pb$ whereas rtg13-mi2 shows lower $^{208}Pb/^{206}Pb$ than RTG301-1. The rtg41-mi1 has higher $^{207}Pb/^{206}Pb$ and $^{208}Pb/^{206}Pb$ than its host rock RTG305. Large filled circles are hypothetical mantle endmembers EM1 and depleted mid-ocean ridge basalt (MORB) source mantle (DMM) projected in $^{208}Pb/^{206}Pb$-$^{207}Pb/^{206}Pb$ space. Shaded area displays variation of bulk-rock Pb isotope compositions of the basalts from Rarotonga Island (Nakamura and Tatsumoto, 1988). (b) Analytical results of olivine-hosted melt inclusions from Rarotonga Island by SIMS (Yurimoto et al., 2004). Error bars are given by 2 SE determined by the statistics of secondary ion intensities. Shaded area displays variation of bulk-rock Pb isotope compositions of the basalts from Rarotonga Island (Nakamura and Tatsumoto, 1988). (c) Results of Independent Component Analysis (ICA) based on the Sr, Nd and Pb isotopic compositions of 6854 terrestrial basaltic rock samples (Iwamori and Nakamura, 2015). Data of southern Pacific OIBs, including samples from Rarotonga Island, are highlighted by a broken line. The values of IC2 range from –4 of HIMU basalt to +4 of EM1 basalts for a limited range of positive IC1. A minor difference arises by omitting Sr and Nd isotopic compositions in the ICA procedure for the Rarotonga bulk-rock compositions (Supplementary Fig. S3), justifying the IC1–IC2 values in this study. One caveat is that such a procedure cannot accurately resolve compositions with an abundant IC3 (~EM2-like) component, which are plotted off the IC1–IC2 plane (Iwamori and Nakamura, 2015). Data of IC1 ≤0.5 should be excluded because they can be MORB rather than OIB. (d) Results of ICA based on the Pb isotope compositions of the two melt inclusions (rtg13-mi2 and rtg41-mi1) in the enlarged IC1–IC2 plane in (c). Analytical results of melt inclusions with error ellipses in (a) are transformed into the IC space. IC1 and IC2 for bulk compositions of the basaltic rocks from Rarotonga Island by Hanyu et al. (2011) were also calculated and plotted for comparison, using the Pb isotopic compositions only. Two sets of ICA results based on (i) the Pb isotopic compositions only (area encircled by broken line) and (ii) the isotopic compositions for Sr and Nd in addition to Pb (shaded area) for reported bulk rock compositions (Nakamura and Tatsumoto, 1988; Hanyu et al., 2011) almost overlap (Fig. S3 in Supplementary material 3), which indicates that (i) may provide a reasonable representation of the mantle isotopic variability.

the data distribution. Inspection of the ICs in the original variable space may lead to geochemical interpretations; in this case, the IC1 compositional vector likely corresponds to parent-daughter fractionation associated with melting and the subsequent radiogenic ingrowth (Iwamori and Nakamura, 2015). Likewise, the IC2 vector corresponds to that associated with aqueous fluid-rock interactions and radiogenic ingrowth. Polynesian OIBs show an extremely wide variation in IC2, from –4 of high μ (μ = $^{238}U/^{204}Pb$: HIMU) basalt to +4 of EM1 basalts for a limited range of positive IC1 (Fig. 3c), suggesting that their sources consist of a package of a subducted and dehydrated slab and the overlying hydrated boundary layer (Iwamori and Nakamura, 2015). On the IC1–IC2 plane, the two melt inclusions and the bulk-rocks are plotted in the first quadrant with positive IC1 and IC2 (Fig. 3d), implying their origin from a source characterized by a long-term enrichment of melt-component (positive IC1) and aqueous fluid component (positive IC2) (Iwamori and Nakamura, 2015). Two clusters are recognized in the bulk-rock data of Rarotonga Island at IC1 ~ 0.5 and $1.1 \leq IC1 \leq 1.6$, and each cluster elongates along IC2 with $1 \leq \Delta IC2 \leq 2$ (Fig. 3d). The rtg41-mi1 is more enriched with aqueous fluid-component (higher IC2) and depleted in melt-component (lower IC1) compared to rtg13-mi2. Such discrimination has become possible owing to high-precision analysis of Pb isotopes by LA-ICP-MS and ICA, which suggests that the mantle source beneath Rarotonga Island is heterogeneous. This study is ongoing and we will add discussion on the effects of crystallization and add analytical data of homogenized melt inclusions. Heating homogenization will ensure implications from trace elements if some diffusive volatile elements are discarded (Hauri, 2002).

Acknowledgments—We thank K. Ohki of OK Lab. Ltd. and S. Sasaki and N. Kanazawa of Thermo Fisher Scientific for their generous support in instrumental development. This project was funded by JSPS KAKENHI Grant Numbers JP15H02148 and JP16H01123 for J.-I.K. and JP26400526 for T.U. Critical reviews by Dr. Shuhei Sakata and an anonymous reviewer improved this manuscript. We are also grateful for the reviews and editorial handling by Professor Tetsu Kogiso.

References

Hanyu, T., Tatsumi, Y., Senda, R., Miyazaki, T., Chang, Q., Hirahara, Y., Takahashi, T., Kawabata, H., Suzuki, K. and Kimura, J.-I. (2011) Geochemical characteristics and origin of the HIMU reservoir: A possible mantle plume source in the lower mantle. *Geochem. Geophys. Geosyst.* **12**, Q0AC09, doi:10.1029/2010GC003252.

Hauri, E. (2002) SIMS analysis of volatiles in silicate glasses, 2: isotopes and abundances in Hawaiian melt inclusions. *Chem. Geol.* **183**, 115–141.

Iwamori, H. and Nakamura, H. (2015) Isotopic heterogeneity of oceanic, arc and continental basalts and its implications for mantle dynamics. *Gondwana Res.* **27**, 1131–1152.

Kimura, J.-I. and Chang, Q. (2012) Origin of the suppressed matrix effect for improved analytical performance in determination of major and trace elements in anhydrous silicate samples using 200 nm femtosecond laser ablation sector-field inductively coupled plasma mass spectrometry. *J. Anal. Atom. Spectrom.* **27**, 1549–1559.

Kimura, J.-I., Chang, Q., Kanazawa, N., Sasaki, S. and Vaglarov, B. S. (2016) High-precision *in situ* analysis of Pb isotopes in glasses using 10^{13} Ω resistor high gain amplifiers with ultraviolet femtosecond laser ablation multiple Faraday collector inductively coupled plasma mass spectrometry. *J. Anal. Atom. Spectrom.* **31**, 790–800.

Nakamura, Y. and Tatsumoto, M. (1988) Pb, Nd, and Sr isotopic evidence for a multicomponent source for rocks of Cook-Austral Islands and heterogeneities of mantle plumes. *Geochim. Cosmochim. Acta* **52**, 2909–2924.

Paul, B., Woodhead, J. D., Hergt, J., Danyushevsky, L., Kunihiro, T. and Nakamura, E. (2011) Melt inclusion Pb isotope analysis by LA-MC-ICPMS: Assessment of analytical performance and application to OIB genesis. *Chem. Geol.* **289**, 210–223.

Rose-Koga, E. F., Koga, K. T., Schiano, P., Le Voyer, M., Shimizu, N., Whitehouse, M. J. and Clocchiatti, R. (2012) Mantle source heterogeneity for South Tyrrhenian magmas revealed by Pb isotopes and halogen contents of olivine-hosted melt inclusions. *Chem. Geol.* **334**, 266–279.

Saal, A. E., Hart, S. R., Shimizu, N., Hauri, E. H., Layne, G. D. and Eiler, J. M. (2005) Pb isotopic variability in melt inclusions from the EM1-EMII-HIMU mantle and-members and the role of the oceanic lithosphere. *Earth Planet. Sci. Lett.* **240**, 605–620.

Sun, S.-s. and McDonough, W. F. (1989) Chemical and isotopic systematics of ocean basalts: implications for mantle composition and processes. *Magmatism in the Ocean Basins* (Sounders, A. D. and Norry, M. J., eds.), *Geol. Soc. Spec. Publ.* **42**, 313–345.

Yurimoto, H., Kogiso, T., Abe, K., Barsczus, H. G., Utsunomiya, A. and Maruyama, S. (2004) Lead isotopic compositions in olivine-hosted melt inclusions from HIMU basalts and possible link to sulfide components. *Phys. Earth Planet. Int.* **146**, 231–242.

Supplementary Materials

URL (http://www.terrapub.co.jp/journals/GJ/archives/data/52/MS497.pdf)
Figures S1 to S3
Tables S1 and S2